



Dependence of the superconducting transition temperature on the doping level in single crystalline diamond films.

Etienne Bustarret, Jozef Kacmarcik, Christophe Marcenat, Etienne Gheeraert, Catherine Cytermann, Jacques Marcus, Thierry Klein

► To cite this version:

Etienne Bustarret, Jozef Kacmarcik, Christophe Marcenat, Etienne Gheeraert, Catherine Cytermann, et al.. Dependence of the superconducting transition temperature on the doping level in single crystalline diamond films.. 2004. <hal-00002689>

HAL Id: hal-00002689

<https://hal.archives-ouvertes.fr/hal-00002689>

Submitted on 24 Aug 2004

HAL is a multi-disciplinary open access archive for the deposit and dissemination of scientific research documents, whether they are published or not. The documents may come from teaching and research institutions in France or abroad, or from public or private research centers.

L'archive ouverte pluridisciplinaire **HAL**, est destinée au dépôt et à la diffusion de documents scientifiques de niveau recherche, publiés ou non, émanant des établissements d'enseignement et de recherche français ou étrangers, des laboratoires publics ou privés.

Dependence of the superconducting transition temperature on the doping level in single crystalline diamond films

E. Bustarret¹, J. Kačmarčík^{2,3}, C. Marcenat³, E. Gheeraert¹, C. Cytermann⁴, J. Marcus¹ and T. Klein^{1,5}

¹ *Laboratoire d'Etudes des Propriétés Electroniques des Solides, CNRS, B.P.166, 38042 Grenoble Cedex 9, France*

² *Centre of Low Temperature Physics IEP SAS & FS UPJŠ, Watsonova 47, 043 53 Košice, Slovakia*

³ *Commissariat à l'Energie Atomique - Grenoble,*

Département de Recherche Fondamentale sur la Matière Condensée,

SPSMS, 17 rue des Martyrs, 38054 Grenoble Cedex 9, France

⁴ *Physics Department and Solid State Institute, Technion, 32000 Haifa, Israel and*

⁵ *Institut Universitaire de France and Université Joseph Fourier, B.P.53, 38041 Grenoble Cedex 9, France*

(Dated: August 5, 2004)

Homoepitaxial diamond layers doped with boron in the $10^{20} - 10^{21} \text{ cm}^{-3}$ range are shown to be type II superconductors with sharp transitions ($\sim 0.2 \text{ K}$) at temperatures increasing from 0 to 2.1 K with boron contents. The critical concentration for the onset of superconductivity is about $5 - 7 \cdot 10^{20} \text{ cm}^{-3}$, close to the metal-insulator transition. The $H - T$ phase diagram has been obtained from transport and a.c. susceptibility measurements down to 300 mK. These results bring new quantitative constraints on the theoretical models proposed for superconductivity in diamond.

PACS numbers: 74.25.Op, 74.63.c, 73.61.Cw

Type II superconductivity has been recently reported for heavily boron-doped polycrystalline diamond prepared either as bulk [1] or thin film samples [2], providing a new interesting system for the study of superconductivity in doped semiconductors. Based on the great bonding strength of the valence band states and on their strong coupling to the carbon lattice phonons, various theoretical studies [3, 4] have stressed the similarity between diamond and the recently discovered MgB_2 system which shows a surprisingly high T_c value on the order of 40 K. Those calculations lead to T_c values in the 0.2 to 25 K range (depending on the boron content) but ignore the boron impurity band [3, 4]. An alternative theoretical approach [5] stresses out the fact that the boron concentration range where superconductivity has been observed is close to the Anderson-Mott metal-insulator transition and suggests an electron correlation driven extended s -wave superconductivity in the boron impurity band.

The open questions of the nature of the metal-insulator transition (MIT) in diamond and of its correlation with superconductivity are of fundamental interest and provide ample motivation for this first investigation of the dependence of the superconducting transition temperature on the doping boron concentration. In this letter, we report on magnetic and transport experiments on a set of high quality single crystalline epilayers doped in the relevant $10^{20} - 10^{21} \text{ cm}^{-3}$ range. We show that T_c rapidly increases above some critical concentration $\sim 5 - 7 \cdot 10^{20} \text{ cm}^{-3}$ reaching $\sim 2 \text{ K}$ for $n_B = 19 \cdot 10^{20} \text{ cm}^{-3}$ (see Table 1).

001-oriented type Ib diamond substrates were first exposed to a pure hydrogen plasma. Methane (4%) was subsequently introduced and a $0.5 \mu\text{m}$ -thick buffer layer of non-intentionally doped material was deposited at 820° C by the microwave plasma-assisted decomposition

TABLE I: Sample characteristics : thickness (t), gas phase ratio $((B/C)_{gas})$, boron concentration (n_B) and critical temperatures (T_c) for the studied diamond epitaxial films

Sample	t (μm)	$(B/C)_{gas}$ (ppm)	n_B (10^{20} cm^{-3})	T_c (K)
1	3.0	1615	3.6	≤ 0.05
2	3.0	1730	9	0.9
3	3.0	1845	10	1.2
4	2.0	2200	11.5	1.4
5	0.15	2800	19	2.1

(MPCVD) of the gas mixture at a total pressure of 30 Torr. Finally, diborane was introduced in the vertical silica wall reactor with boron to carbon concentration ratios in the gas phase $((B/C)_{gas})$ ranging from 1500 to 3000 ppm. With a typical growth rate of $0.9 \mu\text{m/hr}$ these deposition conditions led to 0.1 to $4 \mu\text{m}$ -thick p^+ -type diamond layers. Secondary Ion Mass Spectroscopy (SIMS) depth profiles of $^{11}\text{B}^-$, $^{12}\text{C}^-$ and $^{11}\text{B}^{12}\text{C}^-$ ions were measured using a Cs^+ primary ion beam in a Cameca Ims 4f apparatus. As shown in Fig.1 for samples 2, 4 and 5, these profiles were found to be flat or with a slow decrease toward the buffer layer. The boron atomic densities n_B shown both in Fig.1 and Table 1 were derived from a quantitative comparison to a SIMS profile measured under the same conditions in a B -implanted diamond crystal with a known peak boron concentration of $2.4 \cdot 10^{20} \text{ cm}^{-3}$. For thin enough samples, the profile yielded also the residual doping level in the buffer layer, around 10^{18} cm^{-3} . Moreover, the single crystal and epitaxial character of the MPCVD layers was checked by high resolution X-ray diffraction, yielding shifted narrow lines with smaller linewidths at half maximum than for the Ib substrate (typically 10 arcsec for the 004 Bragg spot of the epilayer, instead of 13 arcsec for the sub-

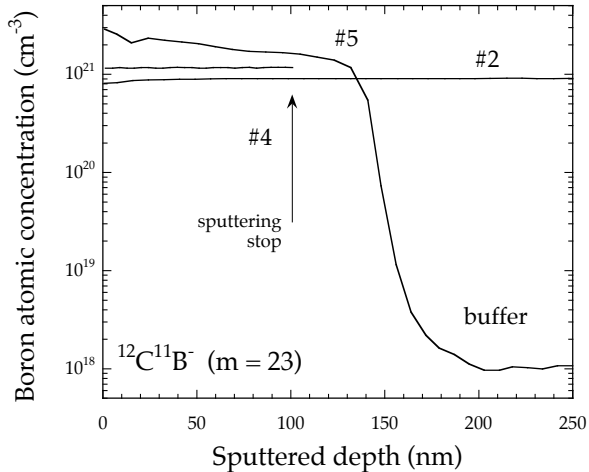


FIG. 1: SIMS profiles for ion mass 23 obtained using Cs^+ primary ions on samples 2, 4 and 5. In the case of the thicker samples, sputtering was interrupted before reaching the buffer layer.

strate). The chemical composition [6], structural [7, 8] and optical [6, 8, 9] characteristics of these layers at room temperature are well documented and have been reviewed recently, together with some preliminary transport measurements [8].

The superconducting temperatures have been deduced from ac-susceptibility measurements (χ_{ac}). The films have been placed on top of miniature coils and T_c has been obtained by detecting the change in the self induction of the coils induced by the superconducting transitions. For fully screening samples, we observed a 4% drop of the induction L (~ 1 mH). Small ac-excitation fields ($\omega \sim 99$ kHz and $h_{ac} \sim$ a few mG) have been applied perpendicularly to the films. Four Au/Ti electrodes were deposited on top of the film with the highest T_c for magneto-transport measurements. A very small current (~ 1 nA) corresponding to a current density on the order of 10^{-3} Acm $^{-2}$ has been used to avoid flux flow dissipation. A standard lock-in technique at 17 Hz was used to measure the temperature dependencies of the sample resistance at fixed magnetic fields. The measurements were performed down to 50 mK (χ_{ac}) and 300mK (transport) and the magnetic field was applied perpendicularly to the doped plane of the sample,

The critical temperatures (see Table 1) reported in Fig.2 have been deduced from the onset of the diamagnetic signal (see inset of Fig.2). The susceptibility has been rescaled to -1 in the superconducting state and a $N \sim 0.9$ demagnetization coefficient has been used (the values of T_c do not depend on this choice). This choice for N leads to a dissipation peak on the order of $0.2 - 0.3$ as expected for the non linear regime. This is consistent with the observation of a slight increase of the width

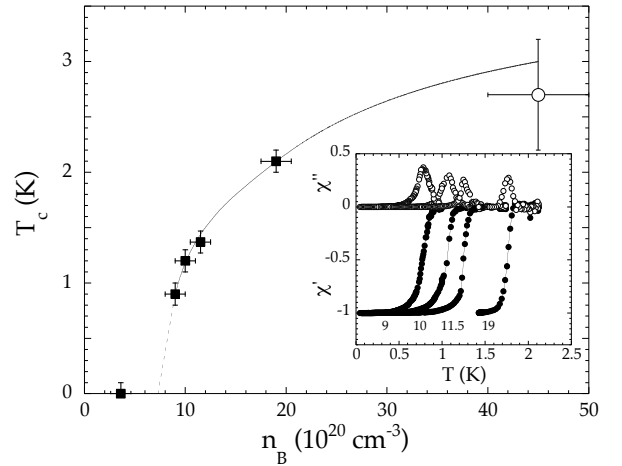


FIG. 2: Dependence of the superconducting transition temperature T_c on the boron concentration n_B : closed squares : this work, open circle : from [1]. The different T_c values were obtained from the onset of the diamagnetic signal (see inset for the real (closed symbols) and imaginary (open symbols) parts of the magnetic susceptibility).

of the transition for increasing h_{ac} values. As shown in the inset of Fig.2 (and Fig.3), the transitions are very sharp (with a width ~ 0.2 K) allowing an accurate determination of T_c and stressing out the high quality of our samples. In comparison, the polycrystalline samples measured in previous reports presented a much larger resistivity transition width, ~ 1.7 K in [1] and ~ 2.6 K in [2].

No transition was observed down to 50 mK for the film with $n_B = 3.6 \cdot 10^{20}$ cm $^{-3}$. For higher boron concentrations, T_c increases rapidly with doping above some critical concentration $\sim 5 - 7 \cdot 10^{20}$ cm $^{-3}$ reaching 2.1 K for $n_B = 19 \cdot 10^{20}$ at.cm $^{-3}$. The dependance of T_c with doping extrapolates towards the data recently obtained by [1]. On the contrary, our T_c value for $n_B \sim 10^{21}$ cm $^{-3}$ (~ 1 K) is much lower than the one recently reported by [2] ($\sim 4 - 7$ K). Our data suggests that these authors have largely underestimated the boron concentration of their polycrystalline samples. They deduced this concentration from Hall measurements which are known to give results that deviate significantly from the actual boron concentration in p^+ -type diamond [7]. It is also worth noticing that we observed superconducting transitions with T_c on the order of 1 K for boron contents ~ 0.5 at.% whereas recent calculations of the electron-phonon coupling led to much smaller T_c values for these doping levels [3-5].

The influence of an external field on the superconducting transition is displayed in Fig.3. As shown in panel a, the transition is shifted towards lower temperatures as the magnetic field is increased. The transition width re-

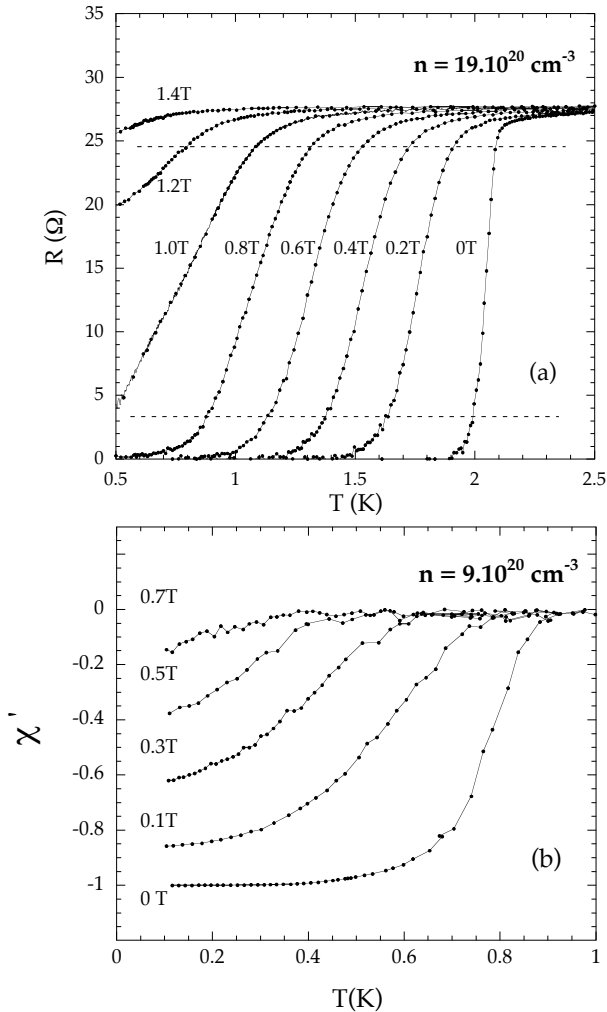


FIG. 3: (a) : temperature dependence of the electrical resistance at indicated magnetic fields for the film with $n = 19.10^{20}$ at.cm $^{-3}$. The dashed lines correspond to the two criteria used for the determination of H_{c2} (see Fig.3) i.e. $R/R_N = 90\%$ and 10% (R_N being the normal state resistance).(b) temperature dependence of the real part of the magnetic susceptibility at indicated magnetic fields for the film with $n = 9.10^{20}$ at.cm $^{-3}$. H_{c2} has been deduced from the onset of the diamagnetic signal.

mains relatively small up to ~ 1 T and rapidly increases for larger fields. In the absence of thermodynamic measurements, some care should be taken in order to define an accurate H_{c2} line. This line has been defined from the classical $R/R_n = 90\%$ criterion (where R_N is the normal state resistance). As shown in Fig.4, the corresponding $H_{c2}(T)$ line can be well described by the classical WHH theory [10]. We hence get $H_{c2}(0) \sim 1.4$ T corresponding to a coherence length $\xi_0 = \sqrt{\Phi_0/2\pi H_{c2}(0)} \sim 150\text{\AA}$ for $n_B = 19 \cdot 10^{20} \text{ cm}^{-3}$ (Φ_0 being the flux quantum). We have also reported on Fig.4 the line corresponding to $R/R_n = 10\%$ which gives an indication for the width

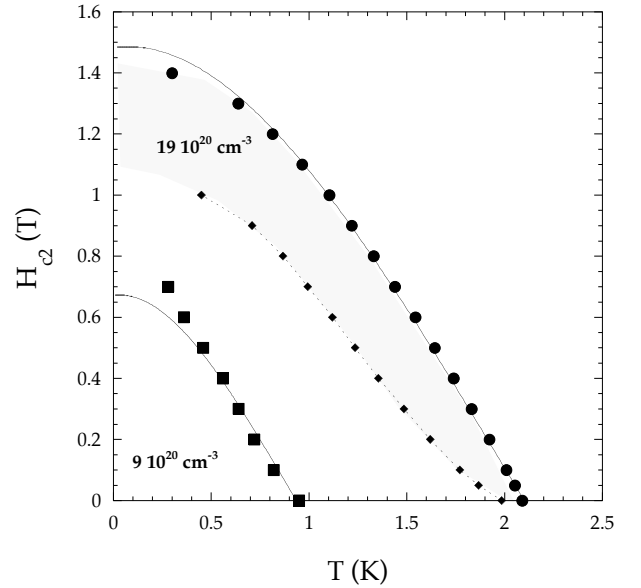


FIG. 4: $H - T$ phase diagram for the films with $n_B = 19 \cdot 10^{20} \text{ cm}^{-3}$ and $n_B = 9 \cdot 10^{20} \text{ cm}^{-3}$. The circles (resp. diamonds) have been deduced from temperature sweeps of the electrical resistance (see fig.2) for $R/R_n = 90\%$ (resp. $R/R_N = 10\%$). The shadowed area is an indication of the width of the transition. The closed squares were defined from the onset of the ac-susceptibility (see Fig.2(b)). The full lines are fits to the data using the classical WHH theory.

of the transition, pointing out that the transition curves rapidly increase for $H > 1$ T. For sample 2, this line has been deduced from the shift of the diamagnetic response with increasing fields. In this case, the rapid broadening of the transition is the hallmark of a small critical current density (J_c) again emphasizing the high quality of our films. Indeed, in the non linear regime, the susceptibility is directly related to $J_c d/h_{ac}$ (where d is a characteristic length scale on the order of the sample thickness) and $J_c \approx h_{ac}/d \sim 1 \text{ Acm}^{-2}$ for $\chi' \sim -0.4$. In this case, no saturation was observed down to 200 mK, indicating some deviation from the classical WHH behaviour. Note that for both samples the slope $[dH_{c2}/dT]_{T \rightarrow 0} \sim 1 \text{ T/K}$, which is almost 2 times smaller than the value reported by Ekimov *et al.* [1].

We obtained an almost temperature-independent normal state resistivity on the order of $0.5 \text{ m}\Omega\cdot\text{cm}$ for $n_B = 19 \cdot 10^{20} \text{ cm}^{-3}$ suggesting that our samples are close to the metal-insulator transition. On the basis of the criterion first proposed by Mott [11] for metal-non metal transitions, which in its final form ($N_c^{1/3} a_H = 0.26$, where a_H is the Bohr radius) has been verified in a wide variety of condensed media [12], the critical concentration in p -type diamond is expected to be around $N_c = 1 - 2 \cdot 10^{20} \text{ cm}^{-3}$ [13]. Limitations to this approach arise from the discrepancies in the values proposed in the literature for

the acceptor Bohr radius a_H , in line with other inconsistencies about the valence band parameters of diamond. From an experimental point of view, extrapolations [14] of the Pearson-Bardeen model [15] have led to N_c values ranging from 1.5 to 3.0 10^{20} cm^{-3} , while different transport measurements have prompted other authors to propose that $N_c \sim 7 \cdot 10^{20}$ cm^{-3} [16]. It is worth noticing that those values have been deduced from room temperature measurements. To the best of our knowledge, the only low temperature estimate ($N_c \sim 40 \cdot 10^{20}$ cm^{-3}) has been proposed by Tschepe *et al.* [17] on the basis of a scaling analysis of the electrical conductivity. However, the absolute conductivity values of their implanted samples are much lower than ours despite larger boron concentrations.

The proximity of a MIT in this system, makes it very favorable for the observation of quantum fluctuation effects. The strength of these fluctuations can be quantified through the quantity $Q_u = R_{eff}/R_Q$ where $R_Q = \hbar/e^2 \sim 4.1$ $\text{k}\Omega$ is the quantum resistance and $R_{eff} = \rho_N/s$ (s is a relevant length scale for these fluctuations [18]). Taking $\rho_N \sim 5 \cdot 10^{-4}$ $\Omega\cdot\text{cm}$ and $s \sim \xi(0) \sim$

150 \AA , we obtain a large Q_u ratio ~ 0.1 indicating that quantum effects may be important in this system. These quantum fluctuations may give rise to the melting of the flux line lattice and thus lead to the rapid broadening of the resistive transitions observed at low T and large H . Another indication for such quantum effects, is the almost temperature-independent mixed state resistivity above 1.2 T as previously observed in other systems with similar Q_u values [19, 20]

To conclude, we were able to prepare highly homogeneous and well characterized boron-doped diamond films in the 10^{20} - 10^{21} cm^{-3} range where superconductivity occurs. The value of the critical concentration for the onset of superconductivity is on the order of 5 – 7 10^{20} cm^{-3} . Boron-doped diamond is an ideal system to study the occurrence of superconductivity close to the metal-insulator transition. As a consequence, quantum effects are expected to play a significant role as suggested by the large quantum resistance ratio $Q_u \sim 0.1$.

We are grateful to F. Pruvost who grew some of the diamond layers and to Dr L. Ortega (Cristallographie, CNRS, Grenoble) for the X-ray diffraction experiments.

-
- [1] E.A. Ekimov, V.A. Sidorov, E.D. Bauer, N.N. Melnik, N.J. Curro, J.D. Thompson, S.M. Stishov, *Nature* **428** 542 (2004).
 - [2] Y. Takano, M. Nagao, K. Kobayashi, H. Umezawa, I. Sakaguchi, M. Tachiki, T. Hatano, H. Kwarada, *cond-mat.0406053*.
 - [3] L. Boeri, J. Kortus, O.K. Andersen, *cond-mat.0404447*.
 - [4] K.W. Lee, W.E. Pickett, *cond-mat.0404547*.
 - [5] G. Baskaran, *cond-mat.0404286*.
 - [6] E. Bustarret, F. Pruvost, M. Bernard, C. Cytermann, C. Uzan-Saguy, *phys. stat. sol. (a)* **186** 203 (2001).
 - [7] E. Bustarret, E. Gheeraert, K. Watanabe, *phys. stat. sol. (a)* **199** 9 (2003).
 - [8] F. Brunet, P. Germi, M. Pernet, A. Deneuve, E. Gheeraert, F. Laugier, M. Burdin, G. Rolland, *Diam. and Relat. Mater.* **7** 869 (1998).
 - [9] F. Pruvost, E. Bustarret, A. Deneuve, *Diam. and Rel. Mater.* **9** 295 (2000).
 - [10] N.R. Werthamer, E. Helfand and P.C. Hohenberg *Phys. Rev.* **147** 295 (1966).
 - [11] N.F. Mott, *Can. J. Phys.* **34** 1356 (1956).
 - [12] P.P. Edwards and M.J. Sienko, *Phys. Rev. B* **17** 2575 (1978).
 - [13] H. Shiomi, Y. Nishibayashi, N. Fujimori, *Jpn J. Appl. Phys.* **30** 1363 (1991); A. S. W. Williams, E. C. Lightowers, A.T. Collins, *J. Phys. C* **3** 1727 (1970).
 - [14] T.H. Borst, O. Weis, *Diam. Relat. Mater.* **4** 848 (1995); J.-P. Lagrange, A. Deneuve, E. Gheeraert, *Diam. Relat. Mater.* **7** 1390 (1998).
 - [15] G.L. Pearson and J. Bardeen, *Phys. Rev. B* **17** 2575 (1978).
 - [16] K. Nishimura, K. Das, J.T. Glass, *J. Appl. Phys.* **69** 3142 (1991).
 - [17] T. Tschepe, J.F. Prins, M.J.R. Hoch, *Diam. Relat. Mater.* **8** 1508 (1999).
 - [18] G. Blatter, B. Ivlev, Y. Kagan, M. Theunissen, Y. Volokitin and P. Kes, *Phys. Rev. B* **50** 13013 (1994).
 - [19] A. Yazdani and A. Kapitulnik, *Phys. Rev. Lett.* **74** 3037 (1995).
 - [20] S. Okuma, Y. Imamoto and M. Morita, *Phys. Rev. Lett.* **86** 3136 (2001).